Characterization of the Avignonet landslide (French Alps) with seismic techniques

D. Jongmans, F. Renalier, U. Kniess, S. Schwartz, E. Pathier & Y. Orengo
LGIT, Université Joseph Fourier, Grenoble Cedex 9, France

G. Bièvre
LGIT, Université Joseph Fourier, Grenoble Cedex 9, France
CETE de Lyon, Laboratoire Régional d'Autun, Autun cedex, France

T. Villemin
LGCA, Université de Savoie, France

C. Delacourt
Domaines Océaniques, UMR6538, IUEM, Université de Bretagne Occidentale, France

ABSTRACT: The large Avignonet landslide (40×10^6 m^3) is located in the Trieves area (French Alps) which is covered by a thick layer of glacio-lacustrine clay. The slide is moving slowly at a rate varying from 1 cm/year near the upper scarp to over 13 cm/year at the toe. A preliminary geophysical campaign was performed in order to test the sensitivity of geophysical parameters to the gravitational deformation. In the saturated clays where the landslide occurs, the electrical resistivity and P-wave velocity are little affected by the slide. On the contrary, S-wave velocity (Vs) values in the first ten meters were found to be inversely correlated with the measured displacement rates along the slope. These results highlight the interest of measuring Vs values in the field for characterising slides in saturated clays and of developing techniques allowing the 2D and 3D imaging of slides.

1 INTRODUCTION

Slope movements in clay formations are world widespread and usually result from complex deformation processes, including internal strains in the landslide body and slipping along rupture surfaces (Picarelli et al. 2004). Such mass movements are likely to generate changes in the geophysical parameters characterizing the ground, which can be used to map the landslide body. Since the pioneering work of Bogoslovsky & Ogilvy (1977), geophysical techniques have been increasingly but still relatively little used (or referenced) for landslide investigation purposes (McCann & Forster 1990, Jongmans & Garambois 2007).

The recent emergence of 2D and 3D geophysical imaging techniques, easy to deploy on slopes and investigating a large volume in a non-invasive way, has made more attractive the geophysical methods for landslide applications. One of the key factors controlling the success of geophysical techniques is the existence of a contrast differentiating the landslide body to be mapped. In the past (Caris & van Asch 1991,

Schmutz et al. 2000, Lapenna et al. 2005, Grandjean et al. 2006, Méric et al. 2007) seismic and electrical methods were successfully used in clay deposits for distinguishing the mass in motion from the unaffected ground.

The aim of this study is to test the sensitivity of the main geophysical parameters (with a focus on the shear wave velocity) to the clay deformation generated by the landslide of Avignonet where geotechnical and geodetic data are available.

2 THE AVIGNONET LANDSLIDE

The large Avignonet slide (40.10^6 m^3) located in the Trieves region (French Alps, Figure 1) was studied. This 300 km^2 area is covered by a thick Quaternary clay layer (up to 200 m) deposited in a glacially dammed lake during the Würm period (Giraud et al. 1991). These clayey deposits overlay compact old alluvial layers and marly limestone of Mesozoic age, and are covered by thin till deposits. After the glacier melting, rivers have cut deeply into the geological
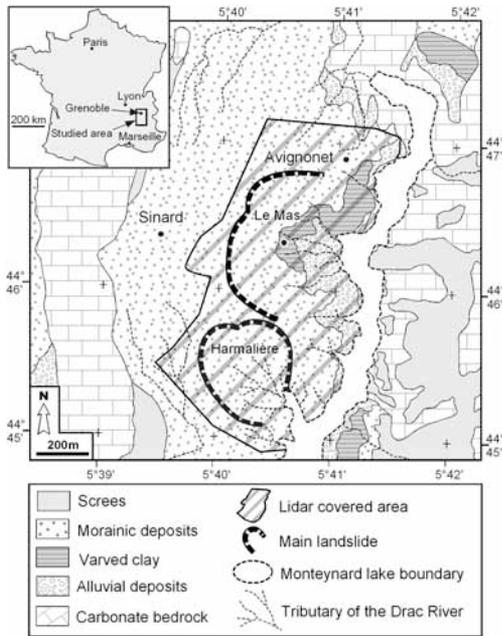
Figure 1. Geological map with the location of the Avignonet and Harmalière landslides, and of the area investigated by Lidar.
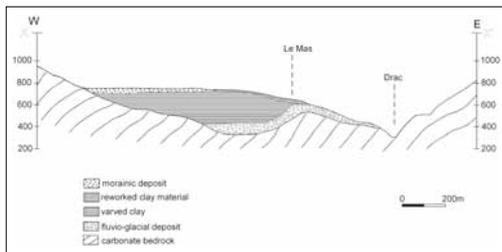

Figure 2. EW geological cross-section over the hamlet of Le Mas (Figure 1.).

formations, triggering numerous landslides (Giraud et al. 1991). Figure 1 shows the simplified geological map of the studied area, in the northern part of the Trièves region, as well as the two main landslides (Avignonet, Harmalière) occurring in the clay deposits. An EW synthetic geological section over the Avignonet landslide is presented in Figure 2, showing the thickness variation of the clay layer, from 0 m to more than 200 m. The translational Avignonet slide, whose first signs of instability were noticed between 1976 and 1981 (Lorier & Desvarreux 2004), affects a surface of about 1×10^6 m^2, with a global eastward motion to the Drac valley which is dammed

downstream. South of this slow moving slide, a quick mudslide (Harmalière, Figure 1) occurred in March 1981, creating a head scarp of 30 m and affecting a surface of about 450,000 m^2 (Moulin & Robert 2004) in the same material. Between 1981 and 2004, the head scarp has continuously regressed with an average of 10 m/year in a north-eastward direction. It now intersects the limit of the Avignonet landslide. The source zone displays complex deformation patterns, including rotational slips, cracks, slumps, and translational failures. In the track and at the toe, the slide evolves into a flow during heavy rainfalls, contributing to the depletion of the landslide mass and the southward erosion process.

3 GEOTECHNICAL AND GEODETIC INVESTIGATION

The Avignonet landslide which affects the hamlet of Le Mas (Figures 1 and 2) was investigated by four boreholes (T0 to T3), equipped with inclinometers (see Figure 4 for location and Table 1 for the main results). The contact with the alluvial deposits was found at 14.5 m, 44.5 m and 56 m in T2, T3 and T1 respectively, whereas T0 was still in the clay deposits at 89 m, in agreement with the westwards thickening of this formation (Figure 2). Inclinometer data revealed several rupture surfaces, at a few m depth (T0 and T2), between 10 m and 17 m (T0, T1, T2, T3) and up to 42 to 47 m (T1 and T0) (Table 1, Lorier & Desvarreux 2004). Of particular importance is the presence of a major active slip surface found at 13 m depth in borehole T2 which is located in the more active area.

Piezometric measurements showed the presence of a very shallow water table (1 to 3 m below the ground level). No geotechnical investigation was performed

Table 1. Borehole and inclinometer results.

	Geological formations	Depth of rupture surface
T0	0–5 m: morainic deposits	5 m
	5–89 m: varved clays	10 m
		47 m
T1	0–5 m: morainic deposits	15 m
	5–56 m: varved clays	34 m
	56–59 m: alluvial deposits	42.5 m
T2	0–4 m: morainic deposits	1.5 m
	4–14.5 m: varved clays	4 m
	14.5–17 m : alluvial deposits	12 m
T3	0–4 m: morainic deposits	16 to 17 m
	4–44.5 m: varved clays	
	44.5–59 m: alluvial deposits	

on the Harmalière landslide which does not threaten any property in the short term.

3.1 Lidar acquisition

A Lidar (Light Detection and Ranging) acquisition, covering the zone displayed in Figure 1, was performed in November 2006 with the handheld airborne mapping system Helimap system® (Vallet & Skaloud 2004). As regards the Lidar, the measurement unit is composed of 3 sensors: a GPS receiver, providing the position of the unit, an inertial measurement unit which provides the orientation of the system, and a laser scanner unit measuring a point cloud of the surface. The height of flight was of 500 m above the ground and allowed to acquire a density of one point by square meter in average. The system displays a high accuracy of ~10 cm both in horizontal and vertical. The interpolated Digital Elevation Model (DEM) is shown in Figure 3 at a resolution of 2 m. The DEM enlightens several landslide indicators. It clearly displays the crescent-shaped front scarp of the Avignonet landslide which intersects the Harmalière one to the South and another minor one to the North.
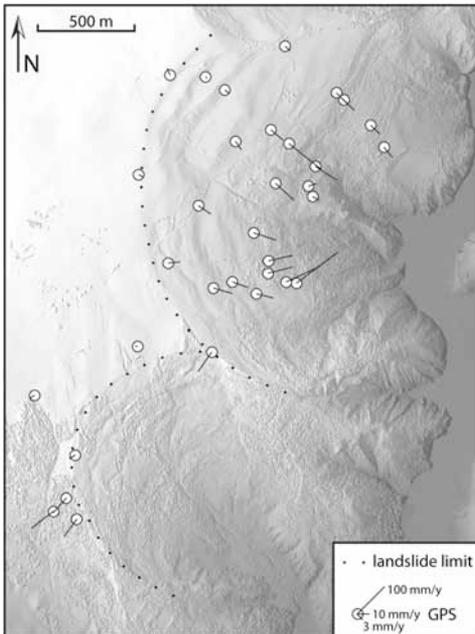

Figure 3. Shaded Lidar-derived DEM of the Avignonet and Harmalière areas acquired from Helicopter. White circles are campaign GPS stations. Black lines indicate mean velocity values measured by GPS from 1995 to present. Dashed lines show the limits of the two landslide.

Inside the Avignonet slide, the DEM shows the presence of multiple parallel scarps down the slope with a spacing of about 100 m. Scarp heights are higher within the slide, suggesting that this latter regresses toward the plateau at the west and that the motion could be greater at the toe than at the crown. In the lower part of the hill, the slope increases due to the presence of consolidated alluvial layers over which the clay material flows (Fig. 2). The geometry of the Harmalière landside is more elongated than the Avignonet one, with a the presence of multiple curved scarps in the source area and a funnel shaped track zone through which the material flows to the lake with a regular slope. To the south-west, the Harmalière landslide also intersects another landslide. This difference in the morphology and in the mechanical behaviour between the two landslides, developing in the same material, probably results from the disappearance of the crest made of bedrock and alluvial layers to the south, removing the buttress that prevents the deep sliding of the Avignonet landslide.

3.2 GPS measurements

The Avignonet slide has been monitored by biannual GPS measurements at 26 geodetic points since 1995, while only 6 points were installed around the Harmalière landslide, due to the strong deformation inside the mass in motion. The locations of the GPS points are shown on a DEM (Figure 3).

The velocity values at the surface of the Avignonet landslide, averaged from the GPS measurements available (Figure 3) increase downhill, varying from 0 to 2 cm/y at the top to more than 13 cm/y in the most active part of the toe. Most of the area is sliding southeastward, parallel to the general slope. In detail, the deformation pattern is complex and velocity and direction of the ground movement are influenced by local geological and morphological features. The concave shape of the river bank below the landslide clearly controls the slope orientation and consequently the slide direction in the lower part of the hill where the displacement vectors rotate. This morphology seems to be linked to the presence of old and consolidated alluvial deposits overlying the bedrock, around which the clay slides (compare Figures 1 and 3). At lower altitudes, the higher slide velocities measured with GPS are accommodated by scarps and bulges spaced by less than 20 m. Strong velocity contrasts are observed along the landslide toe, which seem to be linked to slope angles which are higher in the southern part. The GPS measurement on the ridge between the Harmalière and Avignonet landslides shows that the Harmalière lateral head scarp still actively moves backwards, involving material belonging to the Avignonet landslide. On the contrary, GPS

measurements northwest of the Harmalière landslide exhibit little displacement. Finally, the three GPS points located along the south-western limit shows the presence of another active slide, south of the Harmalière one.

4 GEOPHYSICAL PROSPECTING

A preliminary geophysical campaign was performed in 2006–2007 in order to test the sensitivity of three geophysical parameters (the electrical resistivity ρ, the P-wave seismic velocity Vp and the S-wave seismic velocity Vs) to the deformation resulting from the slide. It turned out that, in such saturated clays, ρ and Vp are strongly influenced by the water level and are little affected by the landslide activity. On the contrary, Vs showed significant variations both vertically and laterally. For this reason, we have focused our study on the Vs measurements.

Shear wave velocity Vs can be measured by a relatively large number of methods including active source techniques (borehole tests, SH-wave refraction tests, surface wave inversion) and ambient vibration techniques (Jongmans 1992, Socco & Jongmans 2004). In the present study we apply the SH seismic refraction tomography method and the surface wave (SW) inversion for deriving Vs values. Seismic refraction tomography consists in inverting the first arrival times picked on all the signals recorded at all geophones for different shots spread along the profile. In the SH case, transverse horizontal ground motions are generated using a sledge hammer hitting laterally a loaded plank as a source. The picked first arrival times are inverted using the Simultaneous Iterative Reconstruction Technique (SIRT, Dines & Lyttle 1979) and provide 2D Vs images.

In the SW method, Rayleigh waves are generated by a vertical shock and are recorded by vertical geophones, together with P waves. SW dispersion curves are computed using the f-k method, which assumes plane wave propagation and no lateral seismic velocity variations (Socco & Strobbia 2004). Dispersion curves are then inverted to get 1D Vs profiles, using the Geopsy software (http://www.geopsy.org).

For this study, we performed five 115 m long seismic profiles (P1 to P5) and two 470 m long profiles (P6 and P7). The profile location is given in Figure 4. For the short profiles, we used 24 vertical geophones (4.5 Hz) and 24 horizontal geophones (14 Hz) spaced by 5 m, for recording Rayleigh waves and SH waves, respectively. Shots were made every 15 m, with two offsets for SW recordings. Figure 5 shows the seismograms generated along profile P1 by a vertical source and a horizontal SH source. In Figure 4a, one can distinguish the P waves from the Rayleigh waves which are inverted for retrieving
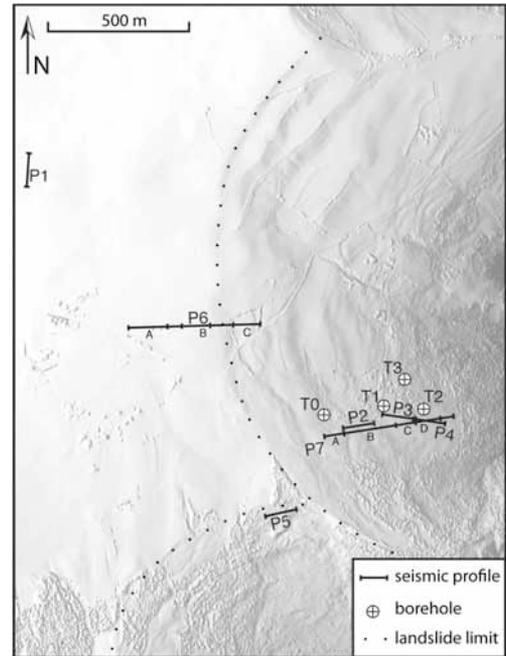

Figure 4. Shaded Lidar-derived DEM with location of the seismic profiles (P1 to P7) and of the boreholes (T0 to T3).
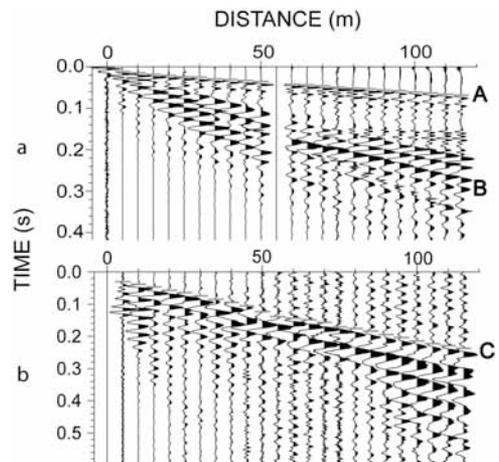

Figure 5. Seismograms along profile P1 for a shot at 0 m. a) Vertical motions generated by a sledge hammer. A: P-wave first arrivals, B: Rayleigh waves. b) Horizontal motions for a SH source. C: SH waves.

the Vs structure. The two long profiles (P6 and P7) were conducted with 48 vertical 4.5 Hz geophones, using explosive sources 80 m and 50 m apart, respectively.

398

4.1 SH tomography

As both SW and refraction travel-time data inversions are non unique problems, we performed a joint analysis of refraction data with surface waves, looking for a common solution in the 1D part of the profiles, with local validation by borehole data (Renalier et al. 2007). Figure 6 shows the Vs images obtained by the SH refraction tomography method for profiles P1, P3 and P5, which are respectively located outside the landslides, on the Avignonet landslide and on the Harmalière landside (Fig. 4). Below profile P1, located on the Sinard plateau, Vs quickly increases to 550 m/s at 5 m depth. Profile P3 exhibits a low-velocity layer (Vs around 250 m/s) with a thickness of 14 m to 19 m from E to W, overlying a more compact layer (Vs > 600 m/s). The depth of this velocity contrast coincides with the slip surface at 13 m found in borehole T2 (Fig. 4). The low Vs values above the slip surface are probably linked to internal strains in the mass resulting from the slide. On the Harmalière landslide (P5), the Vs parameter delineates three distinct layers: a very slow (Vs between 80 and 200 m/s) 5 m thick layer, overlying a 15 m thick layer around 250 m/s, over a more compact layer (Vs > 500 m/s). These results suggest the presence of a slip surface at 20 m deep. SH refraction tomography thus enlightens the evolution of the Vs shallow structure depending on the state of the ground—from undisturbed at P1 to highly disturbed at P5.

4.2 Surface wave interpretation

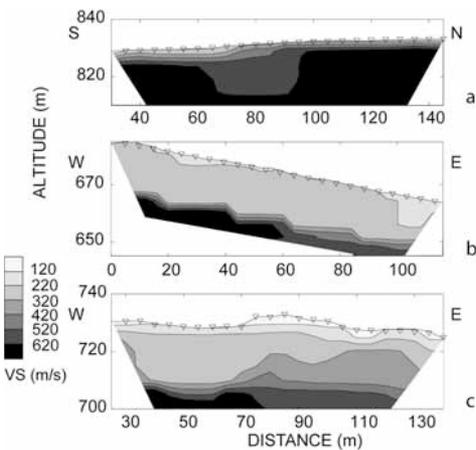Dispersion curves (Rayleigh fundamental mode) for profiles P1, P5, P6 and P7 are plotted in Figure 7. For

Figure 7. Comparison of the phase velocity dispersion curves calculated along profiles P1, P5, P6 and P7.

Figure 6. Vs seismic images (SH refraction tests) along three seismic profiles. a) P1, b) P3 c) P5. RMS values are below 3%.

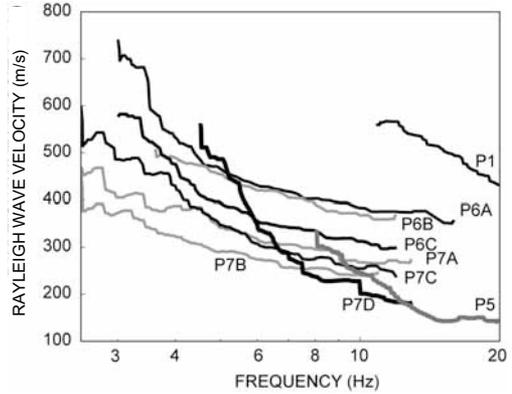the 115 m long profiles P1 and P5, all geophones were considered together. Dispersion curves were computed for both direct and reverse offset shots in order to check the 1D hypothesis. For the 470 m long profiles P6 and P7 seismogram examination and P-wave tomography images were used to define groups of geophones which roughly fit the requirement of 1D media: 3 groups along P6 (from West to East: A: 1–15, B: 19–30, C: 38–48) and 4 groups along P7 (from West to East: A: 1–9, B: 9–28, C: 29–35, D: 35–44). For these groups, dispersion curves were also computed for the two offset shots. All the dispersion curves are gathered on Figure 7.

The two different types of profiles can be easily recognised by their frequency range: dispersion curves for P6 and P7 (explosive sources) exhibit lower frequencies than the curves for P1 and P5 (hammer source). Despite this difference, the Rayleigh wave velocity at high frequency (over 8 Hz) exhibits a significant decrease according to the position of the profile on the two landslides, with the exception of P7C. Rayleigh wave velocities at 14 Hz are divided by 3, from 500 m/s out of the landslides (P1) to 150 m/s on the Harmalière landslide (P5). These results agree with the Vs images of Figure 6. At lower frequencies, the curves do not display such decrease because they are also influenced by the underlying higher velocity alluvial layers and bedrock, which come up from more than 200 m deep on the western part of the studied area, to the surface at the eastern end of the landslides (see Fig. 2).

In a second step, these dispersion curves were inverted using the Neighbourhood Algorithm (Wathelet et al. 2004), giving a two layer Vs model estimate for each group of geophones.
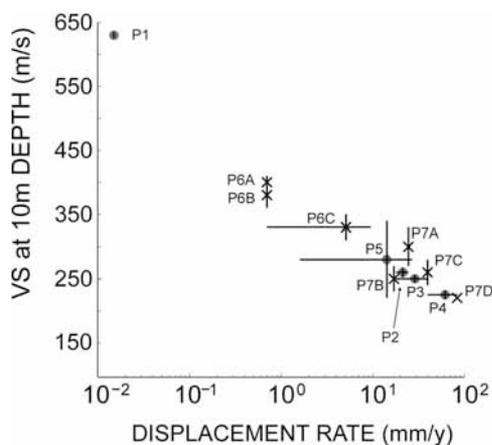
Figure 8. Evolution of shear wave velocity values at 10 m depth with slide velocities. Crosses: surface wave data. Dots: SH refraction data. Vertical error bars on the Vs values are indicated. Horizontal bars indicate the uncertainty range on the displacement rate when no data are available close to the seismic profiles. An arbitrary low displacement rate value of $1\ 10^{-2}$ mm/y has been assumed for profile P1 (Vs = 630 m/s).

4.3 Vs value interpretation

All Vs values obtained by the two methods for each profile or group of geophones are correlated with the displacement rates measured at the GPS points (Fig. 3). For each SH refraction image, two Vs values were extracted at the third and the two thirds of the profile. When no GPS point is close to the seismic profile, the displacement rate is averaged using the two closer data. Figure 7 shows the Vs value with error bars at 10 m depth versus the ground displacement rate in a semi-logarithmic scale. The striking feature is the regular decay of Vs values with the displacement rate, from 630 m/s far from the slide, to 225 m/s at the slide toe, where the slope surface is strongly deformed. These results show that the gravitational deformation strongly affects the shear wave velocity within the clay, which could be used as a parameter for mapping the slide activity.

5 CONCLUSIONS

On the Avignonet landslide, Vs values at shallow depth (10 m) were found to be inversely correlated with displacement rates measured by GPS, with a division by a factor of almost 3 between the zones unaffected and the ones strongly deformed by the landslide. This strong decrease of Vs values is probably linked to internal strains in the mass above the main rupture surface.

Such variations were not observed on P-wave velocity and resistivity values. These results highlight the interest of in-situ measuring Vs values for characterising slides in such saturated clays and of developing techniques allowing the 2D and 3D imaging of landslides. The relationship between Vs values, deformation and pore pressure should be investigated through laboratory tests in order to allow a quantitative interpretation of the field results. Combining Vs imaging with multitemporal remote sensing (satellite and aerial) giving a continuous image of the displacement rates at different times would also allow a deeper insight into the 3D deformation processes and pattern of the landslide. Aerial image archive and new Lidar acquisition planned in autumn 2008 on the Avignonet and Harmalière landslides will supply a global view on the past and present day slide velocity.

REFERENCES

Bogoslovsky, V. & Ogilvy, A. 1977. Geophysycal methods for the inverstigation of landslides. *Geophysics* 42: 562–571.
Caris, J.P.T. & van Asch, T.W.J. 1991. Geophysical, geotechnical and hydrological investigations of a small landslide in the French Alps. *Engineering Geology* 31 (3–4): 249–276.
Dines, K. & Lyttle, J. 1979. Computerized geophysical tomography. *Proceedings of the Institute of Electrical and Electronics Engineers* 67: 1065–1073.
Giraud, A., Antoine, P., van Asch, T.W.J. & Nieyuwenhuis, J.D., 1991, Geotechnical problems caused by glaciolacustrine clays in the French Alps: Engineering Geology 31, 185–195.
Grandjean, G., Pennetier, C., Bitri, A., Méric, O. & Malet, J.P. 2006. Caractérisation de la structure interne et de l'état hydrique de glissements argilo-marneux par tomographie géophysique: l'exemple du glissement-coulée de Super-Sauze. *Comptes Rendus Geosciences* 338 (9): 587–595.
Jongmans, D. 1992. The application of seismic methods for dynamic characterization of soils in earthquake engineering. *Bulletin of the International Association of Engineering Geology* 46 (1): 63–69.
Jongmans, D. & Garambois, S. 2007. Geophysical investigation of landslides: A review. *Bulletin Société Géologique de France* 178 (2): 101–112.

Lapenna, V., Lorenzo, P., Perrone, A., Piscitelli, S., Rizzo, E. & Sdao F. 2005. 2D electrical resistivity imaging of some complex landslides in Lucanian Apennine chain, southern Italy. *Geophysics* 70: B11–B18.

Lorier, L. & Desvarreux, P. 2004. Glissement du Mas d'Avignonet, commune d'Avignonet. *Proceedings of the workshop Ryskhydrogeo, Program Interreg III, La Mure (France)*.

McCann, D.M. & Forster, A. 1990. Reconnaissance geophysical methods in landslide investigations. E*ngineering Geology* 29 (1): 59–78.

Méric, O., Garambois, S., Malet, J-P, Cadet, H., Guéguen P. & Jongmans, D. 2007. Seismic noise-based methods for soft-rock landslide characterization. *Bulletin Société Géologique de France* 178 (2): 137–148.

Moulin, C. & Robert, Y. 2004. Le glissement de l'Harmalière sur la commune de Sinard. *Proceedings of the workshop Ryskhydrogeo, Program Interreg III, La Mure (France)*.

Park, C.B., Miller, R.D. & Xia, J. 1999. Multi-channel analysis of surface waves. *Geophysics* 64 (3): 800–808.

Picarelli, L., Urciuoli, G. & Russo, C. 2004. The role of groundwater regime on behaviour of clayey slopes. *Canadian Geotechnical Journal* 41: 467–484.

Renalier, F., Jongmans, D., Bièvre, G., 'Schwartz, S. & Orengo, Y. 2007. Characterisation of a landslide in clay deposits using Vs measurements. 13th *European Meeting of Environmental and Enginering Geophysics, Istanbul, 3–4 September 2007*.

Schmutz, M., Albouy, Y., Guerin, R., Maquaire, O., Vassal, J., Schott, J.J. & Descloitres, M. 2000. Joint inversion applied to the Super Sauze earthflow (France). *Surveys in Geophysics* 21: 371–390.

Socco, L.V. & Jongmans, D. 2004. Special issue on Seismic Surface Waves. *Near Surface Geophysics* 2: 163–258.

Socco, L.V. & Strobbia, C. 2004. Surface-wave method for near-surface characterization: a tutorial. *Near Surface Geophysics* 2: 165–185.

Vallet, J. & Skaloud J., 2004. Development and Experiences with A Fully-Digital Handheld Mapping System Operated From A Helicopter, The International Archives of the Photogrammetry, Remote Sensing and Spatial Information Sciences, Istanbul, Vol. XXXV, Part B, Commission 5.

Wathelet, M., Jongmans, D. & Ohrnberger, M. 2004. Surface wave inversion using a direct search algorithm and its application to ambient vibration measurements. *Near surface geophysics* 2: 211–221.